AD-A177 168 DYNAMIC FINITE ELEMENT MODELING OF FLEXIBLE STRUCTURES (U) MARYLAND UNIV COLLEGE PARK DEPT OF AEROSPACE ENGINEERING C S CHOI ET AL. 20 NOV 86 AFOSR-TR-87-0165 1/1

UNCLASSIFIED AFOSR-85-0352 F/G 13/13 NL

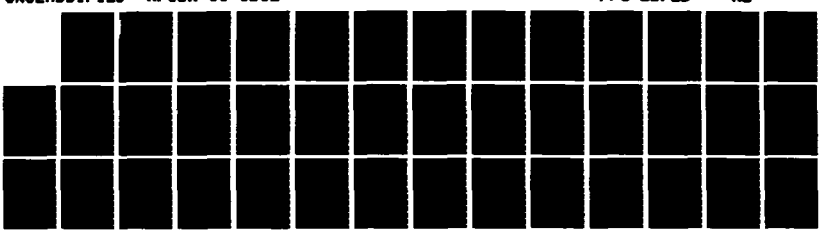

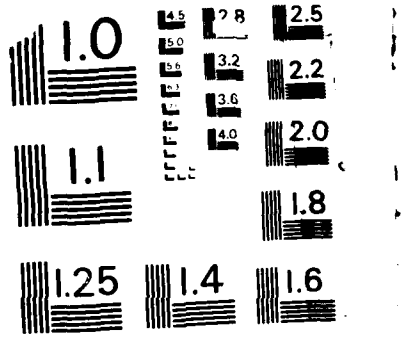

DYNAMIC FINITE ELEMENT MODELING OF FLEXIBLE STRUCTURES

C.S. CHOI

E.R. CHRISTENSEN

S.W. LEE

November 1986

FINAL REPORT

Air Force Office of Scientific Research
Contract No. AFOSR-85-0352

Unclassified
SECURITY CLASSIFICATION OF THIS PAGE

AD-A177 [illegible]

REPORT DOCUMENTATION PAGE

1a. REPORT SECURITY CLASSIFICATION: Unclassified	1b. RESTRICTIVE MARKINGS
2a. SECURITY CLASSIFICATION AUTHORITY	3. DISTRIBUTION/AVAILABILITY OF REPORT: Approved for public release, distribution unlimited
2b. DECLASSIFICATION/DOWNGRADING SCHEDULE	
4. PERFORMING ORGANIZATION REPORT NUMBER(S)	5. MONITORING ORGANIZATION REPORT NUMBER(S): AFOSR-TR-87-0165
6a. NAME OF PERFORMING ORGANIZATION: Department of Aerospace Eng. University of Maryland; 6b. OFFICE SYMBOL (If applicable)	7a. NAME OF MONITORING ORGANIZATION: AFOSR
6c. ADDRESS (City, State and ZIP Code): College Park, Maryland 20742	7b. ADDRESS (City, State and ZIP Code): Bolling AFB Washington, D.C. 20332-6448
8a. NAME OF FUNDING/SPONSORING ORGANIZATION: AFOSR; 8b. OFFICE SYMBOL (If applicable): NA	9. PROCUREMENT INSTRUMENT IDENTIFICATION NUMBER: AFOSR-85-0352
8c. ADDRESS (City, State and ZIP Code): Bolling AFB Washington, D.C. 20332-6448	10. SOURCE OF FUNDING NOS.

PROGRAM ELEMENT NO.	PROJECT NO.	TASK NO.	WORK UNIT NO.
61102F	2302	B1	

11. TITLE (Include Security Classification): Dynamic Finite Element Modeling of Flexible Structures

12. PERSONAL AUTHOR(S): C.S. Choi, E.R. Christensen, S.W. Lee

13a. TYPE OF REPORT	13b. TIME COVERED	14. DATE OF REPORT (Yr., Mo., Day)	15. PAGE COUNT
Final	FROM 9/1/85 TO 2/23/86	Nov. 20, 1986	38

16. SUPPLEMENTARY NOTATION

17 COSATI CODES		
FIELD	GROUP	SUB. GR.

18. SUBJECT TERMS (Continue on reverse if necessary and identify by block number): Reduced basis technique, finite element modeling, space structures, deployments, large deflection

19. ABSTRACT (Continue on reverse if necessary and identify by block number)

In Part I, reduced basis techniques are applied to the problem of the nonlinear analysis of the dynamics of unrestrained flexible structures. The reduced bases used consisted of mode shapes of the structure as well as some modal derivatives. The technique was tested on a simple spacecraft structure. The numerical results indicated that the technique did not appear very promising for this type of problem.

In Part II, a finite element technique is used for analysis of very flexible structures undergoing deployment manuevers. The structure is assumed to consist of flexible bars attached to a rigid mass. The description of elastic deformation is based on the total Lagrangian formulation which allows finite rotation. Numerical tests demonstrates the validity of the present approach.

20 DISTRIBUTION/AVAILABILITY OF ABSTRACT	21. ABSTRACT SECURITY CLASSIFICATION
UNCLASSIFIED/UNLIMITED ☒ SAME AS RPT. ☐ DTIC USERS ☐	Unclassified

22a. NAME OF RESPONSIBLE INDIVIDUAL	22b. TELEPHONE NUMBER (Include Area Code)	22c. OFFICE SYMBOL
Dr. A.K. Amos	(202)767-4937	AFOSR/NA

DD FORM 1473, 83 APR — EDITION OF 1 JAN 73 IS OBSOLETE.

Unclassified
SECURITY CLASSIFICATION OF THIS PAGE

AFOSR-TR- 87-0165

DYNAMIC FINITE ELEMENT MODELING OF FLEXIBLE STRUCTURES

C.S. CHOI

E.R. CHRISTENSEN

S.W. LEE

November 1986

FINAL REPORT

Air Force Office of Scientific Research
Contract No. AFOSR-85-0352

ABSTRACT

In Part I, reduced basis techniques are applied to the prob·m of the nonlinear analysis of the dynamics of unrestrained flexible structures. The reduced bases used consisted of mode shapes of the structure as well as some modal derivatives. The technique was tested on a simple spacecraft structure. The numerical results indicated that the technique did not appear very promising for this type of problem.

In Part II, a finite element technique is used for analysis of very flexible structures undergoing deployment maneuvers. The structure is assumed to consist of flexible bars attached to a rigid mass. The description of elastic deformation is based on the total Lagrangian formulation which allows finite rotation. Numerical tests demonstrates the validty of the present approach.

PART I

A REDUCED BASIS TECHNIQUE FOR THE NONLINEAR ANALYSIS OF THE DYNAMICS OF UNRESTRAINED FLEXIBLE STRUCTURES

1. INTRODUCTION

For large lightweight spacecraft which are undergoing certain types of manuevers such as slewing motions for retargeting or rapid large angle reorientations, large elastic deformations as well as large rigid body motions can occur. These large deformations will be coupled with the rigid body motions resulting in a complicated set of nonlinear differential equations of motion. Applying a finite element approximation to such a problem for a complicated structure results in a system of equations involving a large number of degrees of freedom [1]. In order to avoid using excessive amounts of computer time, it is desirable to reduce the number of unknowns using some sort of reduction method. One method is to apply the classical Rayleigh-Ritz approximation to the system of matrix equations resulting from the finite element discretization [2] thus combining the modeling versatility of the finite element method with the reduction in variables due to the Rayleigh-Ritz method. The accuracy of the reduction method depends of course upon the choice of Rayleigh-Ritz approximation functions or basis vectors. According to [3], these basis vectors should satisfy the following criteria:

(1) The vectors must be linearly independent and span the space of solutions in the neighborhood of the point considered on the solution path.

(2) Their generation should be simple and computationally inexpensive.

(3) They must have good approximation properties in the sense that they provide highly accurate solutions on a large interval of the solution path.

For the solution of static problems, Noor [2,3] has recommended the use of a nonlinear solution and its various order path derivatives as basis vectors. Chan and Hsiao [4] have investigated the use of a normalized set of correction vectors derived during the course of a nonlinear analysis step as the basis vectors for geometrically as well as materially nonlinear static problems. For nonlinear dynamic problems, modal superposition techniques are a popular reduction method [5-11]. These techniques are based in part upon the principle of local mode superposition [12] which states that small harmonic motions may be superimposed upon large displacements and that small forced motion may be represented in terms of the nonlinear (tangent stiffness) frequency spectrum. Nickell [5] and Resmeth [6] have used a modal reduction technique in which the modes and frequencies are updated at each time step in the solution. This approach requires a repeated solution of the free vibration eigenvalue problem. Other investigators [7-11] suggest using the initial eigenvalues throughout the analysis. The nonlinearities must then be taken into account by a psuedo force approach in which the nonlinear terms are included in the force terms on the right hand side of the equation. Bathe and Graceuski [11] recommend this approach for problems with small or local nonlinearities. Noor [3] has reported favorable results using a combination of mode shapes expanded about the unloaded equilibrium configuration and a set of mode shapes expanded about the nonlinear static solution. Wilson et. al [13,14] have used a sequence of orthodgonal Ritz Vectors as a reduced basis for linear dynamics problems. Their approach requires that the loading terms be factored into a sum of space vector multiplied by time functions.

Idelsohn and Cardona [15,16] have shown that for highly nonlinear dynamic systems such as vibrating cantilevered beams that modal superposition techniques require an updating of the basis too frequently and lead to inaccurate results. They reported improved results with not only the tangent eigenmodes but also

some derivatives of them with respect to the modal amplitude parameters as the basis vectors.

All of the work mentioned above has been involved with fully restrained structures. The objective of this report, therefore, is to study the use of reduced basis techniques in the solution of problems dealing with nonlinear unrestrained flexible structures such as those studied in [1].

2. MATHEMATICAL FORMULATION

2.1 Equations of Motion

The motion of an unrestrained flexible body can be described by the following three sets of equations:

1. The conservation of linear momentum
2. The conservation of angular momentum
3. An equation describing the deformations

The finite element equations of motion for an unrestrained deformable body undergoing large deformations have been derived in [1]. The equations evaluated at time t_n are

$$\underset{\sim}{M}^n \ddot{\underset{\sim}{q}}^n + \underset{\sim}{F}_E(\underset{\sim}{q}^n) = \underset{\sim}{F}(\underset{\sim}{q},\dot{\underset{\sim}{q}}) \tag{2.1}$$

The modal displacements including the rigid body ones are denoted by $\underset{\sim}{q}$. The mass matrix is $\underset{\sim}{M}$ and $\underset{\sim}{F}$ is the applied force term. The vector of internal modal forces is $\underset{\sim}{F}_E(\underset{\sim}{q})$ which is a nonlinear function of the modal displacements. Eq. (2.1) is nonlinear and can be solved by a modified Newton-Raphson interations. Letting subscript i represent the ith iteration, eq. (2.1) can be written as

$$\underset{\sim}{M}^n \ddot{\underset{\sim}{q}}^n_{i+1} + \underset{\sim}{K}_T \Delta \underset{\sim}{q}^n_i = \underset{\sim}{F}^n_{T_i} \tag{2.2}$$

where

$$\Delta \underset{\sim}{q}^n_i = \underset{\sim}{q}^n_{i+1} - \underset{\sim}{q}^n_i \tag{2.3}$$

$$\underset{\sim}{F}^n_{T_i} = \underset{\sim}{F}^n_i - \underset{\sim}{F}^n_{s_i} \tag{2.4}$$

$\underset{\sim}{K}_T$ is the tangent stiffness matrix and $\underset{\sim}{F}_s$ is the initial stress force vector. Eq. (2.2) can be integrated timewise using an implicit scheme based on the trapizoidal rule [1]. For a large system, the cost of this computation can be substantial. Reduced basis techniques will be applied to Eq. (2.2) in an effort to reduce those costs.

2.2 Reduced Equations

The Rayleigh-Ritz technique is applied to Eq. (2.2) by approximating g^n_i as follows:

$$\Delta g^n_i = \underset{\sim}{\Gamma} \Delta \underset{\sim}{X}^n_i \tag{2.5}$$

where

$$\underset{\sim}{\Gamma} = [\psi_1 \; \psi_2 \; \cdots \; \psi m] \tag{2.6}$$

$\underset{\sim}{\Gamma}$ is a matrix made up of m linearly independent basis vectors $\psi_1, \psi_2, \ldots, \psi m$ where m is much less than the total number of degrees of freedom for the problem. The vector $\underset{\sim}{X}^n$ represents m undetermined coefficients which must be solved for from the rduced equations. From Eq. (2.5),

$$\dot{g}^n_i = \underset{\sim}{\Gamma} \dot{\underset{\sim}{X}}^n_i \tag{2.7}$$

and

$$g^n_{i+1} = \underset{\sim}{\Gamma} \underset{\sim}{X}^n_{i+1} \tag{2.8}$$

Substituting Eqs. (2.5), (2.7) and (2.8) into Eq. (2.2) and multiplying through by $\underset{\sim}{\Gamma}^T$ results in

$$\overline{\underset{\sim}{M}}^n \ddot{\underset{\sim}{X}}^n_{i+1} + \overline{\underset{\sim}{K}}^n_T \Delta \underset{\sim}{X}^n_i = \overline{\underset{\sim}{F}}^n_{T_i} \tag{2.9}$$

where

$$\overline{\underset{\sim}{M}}^n = \underset{\sim}{\Gamma}^T \underset{\sim}{M}^n \underset{\sim}{\Gamma} \tag{2.10}$$

$$\overline{\underset{\sim}{K}}_T^n = \underset{\sim}{\Gamma}^T \underset{\sim}{K}_T^n \underset{\sim}{\Gamma} \tag{2.11}$$

$$\overline{\underset{\sim}{F}}_{T_i}^n = \underset{\sim}{\Gamma}^T \underset{\sim}{F}_{T_i}^n \tag{2.12}$$

Eq. (2.9) is the reduced set of m equations which are solved timewise by the same scheme as in [1]. Note, however, that since $\underset{\sim}{F}_T = \underset{\sim}{F}_T(\underset{\sim}{q},\dot{\underset{\sim}{q}})$, it is necessary to transform back to the full coordinates via Eq. (2.5) after each iteration in order to recalculate $\underset{\sim}{F}_T$ for the next iteration.

3. SELECTION OF REDUCED BASIS VECTORS

The most difficult and critical part of the reduced basis technique is choosing what vectors to use as a basis. Two different choices of vectors were considered in this study. One choice consisted of a modal method in which the basis vectors consisted of the system eigenvectors. For the other choice, some eigenvector derivatives were added to the basis. Both of these methods are described in more detail below.

3.1 Modal Method

The use of this method is very similar to the use of modal superposition for a linear problem. The basis vectors consist of the first few modes,

$$\underset{\sim}{\Gamma} = \underset{\sim}{\Phi} \tag{3.1}$$

where $\underset{\sim}{\Phi}$ is an Nxm matrix consisting of the m eigenvectors $\phi_1, \phi_2, \ldots, \phi_m$, that is,

$$\underset{\sim}{\Phi} = [\phi_1 \; \phi_2 \; \cdots \; \phi_m] \tag{3.2}$$

Unlike the linear problem, however, the $\underset{\sim}{K}_T$ and $\underset{\sim}{M}$ matrices will not in general be diagonal since the $\underset{\sim}{K}_T$ and $\underset{\sim}{M}_G$ matrices are changing with time. The eigenvectors are found by solving the linearized eigenvalue problem,

$$(\underset{\sim}{K}_T^n - \omega^2 \underset{\sim}{M}^n)\, \underset{\sim}{\phi}_r = 0 \qquad r=1,2,\ldots m \tag{3.3}$$

The eigenvectors can be found from Eq. (3.3) using any method. Since the problems in this study didn't involve a large number of degrees of freedom, the Jacobi method was used to calculate all the modes. For larger problems, more efficient schemes such as subspace iteration or Lanczos method should be used.

3.2 Modal Derivatives Method

Because the problem is nonlinear, the actual eigenvalues and eigenvectors will be functions of the displacements $\underset{\sim}{g}_G$, or alternatively, they will be functions of the modal participation factors $\underset{\sim}{z}$. Thus,

$$\underset{\sim}{\phi}_r = \underset{\sim}{\phi}_r(\underset{\sim}{z}) \tag{3.4}$$

and

$$\Delta \underset{\sim}{g}_G = \sum_{r=1}^{m} \underset{\sim}{\phi}_r(\underset{\sim}{z}) z_r \tag{3.5}$$

If Eq. (3.4) is expanded in a Taylor series around the reference position of $\underset{\sim}{g}_G^n$,

$$\underset{\sim}{\phi}_r = \underset{\sim}{\phi}_r^n + \sum_{s=1}^{m} \left(\frac{\partial \underset{\sim}{\phi}_r}{\partial z_s}\right)^n \Delta z_s + \ldots \tag{3.5}$$

In the modal method it is the first term of the Taylor series which is used as a basis. In the modal derivative method some of the modal derivatives are added to the basis so that

$$\underset{\sim}{\Gamma} = \left[\underset{\sim}{\phi}_1 \ldots \underset{\sim}{\phi}_m \frac{\partial \underset{\sim}{\phi}_1}{\partial z_1} \ldots \frac{\partial \underset{\sim}{\phi}_r}{\partial z_s}\right] \tag{3.6}$$

We needn't add all of the modal derivatives to the basis, the choice of which

ones to keep will depend upon the particular problem being solved. By including these extra terms from the Taylor series in the basis a more accurate representation of the response may be obtained.

The modal derivatives can be found by differentiating Eq. (3.3) with respect to the modal amplitude z_s [16] and then solving the following set of equations [17]:

$$(\underset{\sim}{K}_T - \omega^2 \underset{\sim}{M})^* \frac{\partial \underset{\sim}{\phi}_r^*}{\partial z_s} = \underset{\sim}{f}_{rs}^* \tag{3.7}$$

where

$$\underset{\sim}{f}_{rs} = \underset{\sim}{M}\underset{\sim}{\phi}_r(\underset{\sim}{\phi}_r^T \frac{\partial \underset{\sim}{K}_T}{\partial z_s} \underset{\sim}{\phi}_r) - \frac{\partial \underset{\sim}{K}_T}{\partial z_s} \underset{\sim}{\phi}_r \tag{3.8}$$

The * denotes the matrix and vector obtained by deleting the kth row and column where k is selected such that the absolute value of the kth component of $\underset{\sim}{\phi}_r$ is a maximum. The derivative of the stiffness matix is found as follows [16]:

$$\frac{\partial \underset{\sim}{K}_T}{\partial z_s} = \sum_{j=1}^{N} \underset{\sim}{\phi}_{sj} \frac{\partial \underset{\sim}{K}_T}{\partial q_j} \tag{3.9}$$

Thus in order to determine the modal derivatives it is necessary to calculate the derivative of the stiffness matrix with respect to all the modal displacements.

4. NUMERICAL RESULTS

Both the modal method and the modal derivative method is applied to the sample problem illustrated in Fig. 1. A simple spacecraft consisting of a rigid mass and a flexible beam appendage is subjected to a sinusoidally varying moment applied to the rigid mass. The frequency of the applied moment is equal to the first bending frequency for the undeformed structure. The beam was modelled by two of the three node beam elements developed in [1] which resulted in 13 total unknown degrees of freedom, including the rigid body rotation angle of the rigid

mass. The equations of motion were integrated using a time step size of 0.01 sec. The numerical results for each case are presented below.

4.1 Modal Method

The results using various number of modes in the reduced basis are shown in Fig. 2 where the lateral tip displacement of the beam is plotted as a function of time. The first case considered uses five modes in the basis: One rigid body, the first two bending modes and the first two axial modes. In the second case considered the basis consisted of nine vectors: the rigid body mode plus four bending and four axial modes. The original basis was used throughout the computations for these two cases. The third case considered used three modes, one rigid body and two bending modes as the reduced basis. For this case, however, the three modes were recomputed at each time step.

From Fig. 2 it can be seen that in none of the non-updated cases were the reduced equations sufficient to follow the true response of the complete system. The more modes included in the basis, the better the results, but eventually the results become inaccurate, even with nine modes used in the basis. The results were much better when the modes were updated at each time step, but this entailed a great deal of extra computational expense. Also, the truncation errors due to repeated change of basis accumulated so that eventually the results even for this case were in error.

4.2 Modal Derivative Method

In addition to using some modes in the reduced basis, some modal derivatives are also added. The results for these cases are pictured in Fig. 3. The first case considered included a total of five basis vectors - one rigid body mode, the first two bending modes and the derivatives of the first bending mode with respect to its own amplitude and with respect to the second bonding modes amplitude. The second case considered included 9 basis vectors - the first five

modes (one rigid body + first four bending) plus four modal derivatives, the derivatives of the first bending mode with respect to the amplitudes of bending modes one, two, and three plus the derivative of the second bending mode with respect to its own amplitude.

From Fig. 3, however, it does not appear that the addition of the modal derivatives has improved the results very much. In fact, by comparing Fig.'s 2 and 3, it appears that the results depend upon the total number of basis vectors included rather than upon their nature.

5. CONCLUSIONS

From the numerical results obtained in this study it appears that the use of a reduced basis technique for the solution of the type of problems studied here is not very promising. It may be possible that a different choice of basis vectors would give improved results.

The best results were obtained by updating the modes at each time step. However, this procedure involves considerable computational expense. In addition, the truncation error buildup due to the repeated change of basis eventually led to large errors.

It appears for this type of structure modelled by the type of elements used here that the changes in the modal properties are large enough that reduced basis techniques are not practical due to the large number of basis updatings necessary to accurate model the response.

REFERENCES (PART I)

1. Christensen, E.R., Lee, S.W., "Nonlinear Finite Element Modeling of the Dynamics of Unrestrained Flexible Structures," to appear in Computers and Structures.

2. Noor, A.K., Peters, J.M., "Reduced Basis Technique for Nonlinear Analysis of Structures," AIAA Journal, Vol. 18, No. 4, April 1980, pp. 455-462.

3. Noor, A.K., "Recent Advances in Reduction Methods for Nonlinear Problems," Computers and Structures, Vol. 13, 1981, pp. 31-44.

4. Chan, A.S.L., Hsiao, K.M., "Nonlinear Analysis Using a Reduced Number of Variables," Computer Methods in Applied Mechanics and Engineering, Vol. 55, 1985, pp. 899-913.

5. Nickell, R.E., "Nonlinear Dynamics by Mode Superposition," Computer Methods in Applied Mechanics and Engineering," Vol. 7, 1976, pp. 107-129.

6. Remseth, S.N., "Nonlinear Static and Dynamic Analysis of Framed Strutures," Computers and Structures, Vol. 10, pp. 879-897, 1979.

7. Molnar, A.J., Vashi, K.M., Gay, C.W., "Application of Normal Mode Theory and Pseudoforce Methods to Solve Problems with Nonlinearities," Journal of Pressure Vessel Technology, May 1976, pp. 151-156.

8. Morris, N.F., "The Use of Modal Superposition in Nonlinear Dynamics," Computers and Structures, Vol. 7, pp. 65-72, 1977.

9. Shah, V.N., Bohm, G.J., Nahavandi, A.N., "Modal Superposition Method for Computationally Economical Nonlinear Structural Analysis," Journal of Pressure Vessel Technology, Vol. 101, May 1979, pp. 134-140.

10. Geschwindner, L.F., "Nonlinear Dynamic Analysis by Modal Superposition," JOurnal of the Structural Division, Proceedings of the ASCE, Vol .107, No. ST12, Dec. 1981, pp. 2325-2336.

11. Bathe, K.J., Graceuski, S., "On Nonlinear Dynamic Analysis Using Substructuring and Mode Superposition," Computers and Structures, Vol. 13, pp. 699-707, 1981.

12. Stoker, J.J., Nonlinear Vibrations in Mechanical and Electrical Systems, Interscience Publishers, Inc. N.Y., 1950.

13. Wilson, E.L., Yuan, M., Dickens, J.M., "Dynamic Analysis by Direct Superposition of Ritz Vectors," Earthquake Engineering and Structural Dynamics, Vol. 10, 813-821, 1982.

14. Bayo, E.P., Wilson, E.L., "Use of Ritz Vectors in Wave Propagation and Foundation Response," Earthquake Engineering and Structural Dynamics, Vol. 12, pp. 499-505, 1984.

15. Idelsohn, S.R., Cardona, A., "A Load Dependent Basis for Reduced Nonlinear Structural Dynamics," Computers and Structures, Vol. 20, No. 1-3, pp. 203-210, 1985.

16. Idelsohn, S.R., Cardona, A., "A Reduction Method for Nonlinear Structural Dynamic Analysis," Computer Meth. in Applied Mechanics and Engineering, Vol. 49, 1985, pp. 253-279.

17. Nelson, R.B., "Simplified Calculations of Eignevector Derivatives," AIAA Journal, Vol. 14, No. 9, pp. 1201-1205, September 1976.

Fig. 1

Sample Spacecraft and Loading

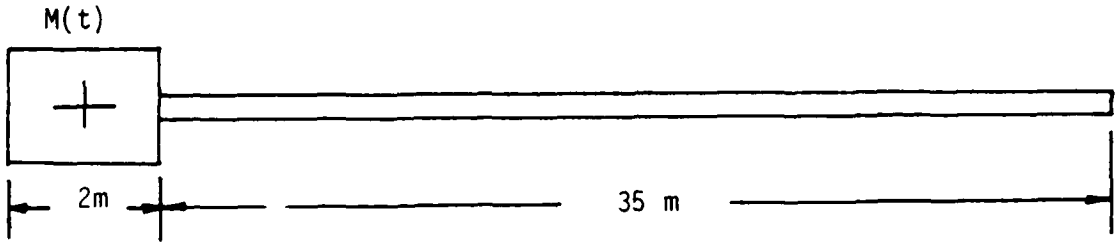

$M(t) = M_0 \sin \omega_0 t$

$M_0 = 10^6$ N-m

$\omega_0 = 8.77$ Rad/sec

Beam Properties:

$E = 3(10^{10})$ N/m^2

$G = 1.154(10^{10})$ N/m^2

Shear Factor = 0.83333

$\rho = 10^3$ Kg/m^3

$A = 0.25$ m^2

$I_{yy} = I_{zz} = 5.0(10^{-3})$ m^4

Rigid Mass Properties:

$m_0 = 7000$ Kg

$I_0 = 5.25(10^4)$ Kg-m^2

Fig. 2

MODAL BASIS ONLY

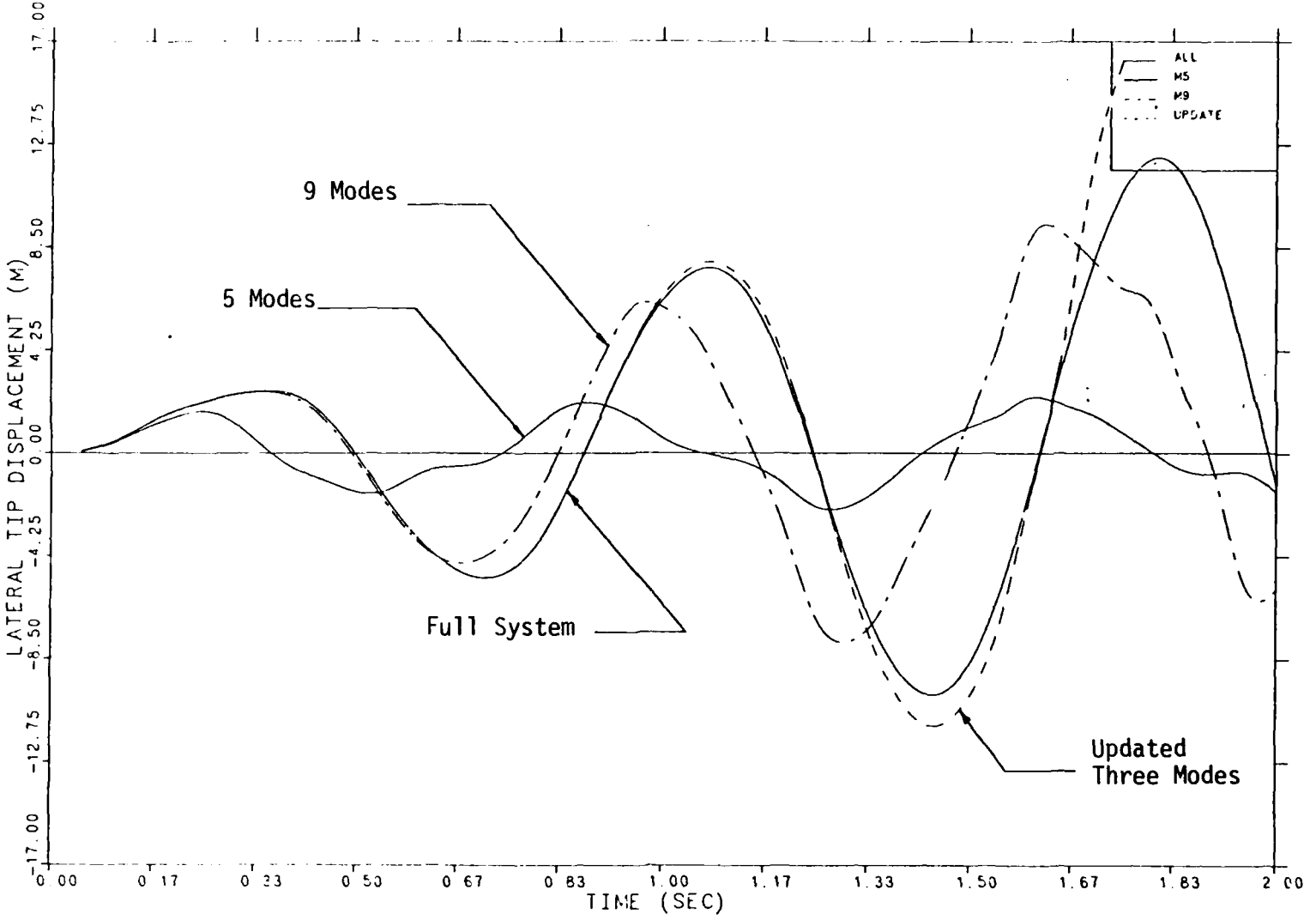

Fig. 3

MODES PLUS MODAL DERIVATIVES INCLUDED IN BASIS

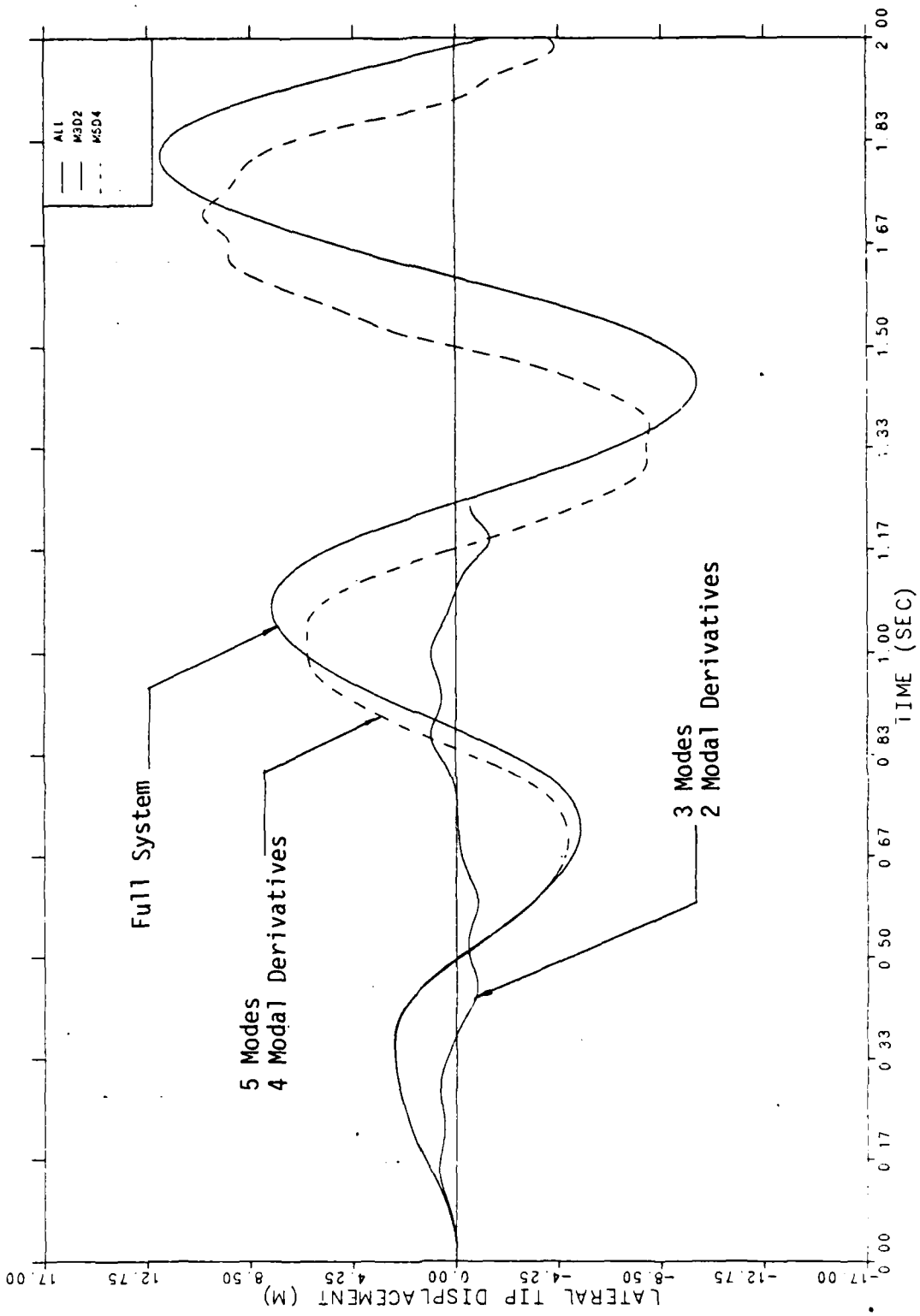

PART 2

FINITE ELEMENT MODELING OF DEPLOYMENT DYNAMICS OF SPACE STRUCTURES

1. INTRODUCTION

The objective of the research project has been to develop an efficient finite element analysis technique for study of deployment and retraction dynamics of large flexible space structures in earth orbit.

With the advent of the space shuttle, it has become feasible to construct a large space structure which can be used as permanent communication and observation posts. However, due to its enormous size, a typical space structure cannot fit into the cargo bay of the current-generation space shuttle in fully deployed mode. Instead it must be folded into a much smaller volume for efficient stowage. Once placed in earth orbit, the space structure is separated from the shuttle and deployed into full dimension for operational use. Also full or part of the space structure may undergo a series of deployment and retraction manuevers as a part of normal operation. Large change in geometrical configuration of space structures during deployment, retraction and other maneuvers implies large change in inertia properties and coupling between gross rigid body motion and elastic deformation. In particular space structures are extremely flexible due to minimum weight requirement and thus are likely to experience large elastic deflection.

Design of space structures requires a very accurate and reliable analysis technique. This is due to the fact that extremely large size of space structures and zero gravity environment make any full-scale test on ground practically impossible. Therefore more reliance on small-scale testing and theoretical analysis is inevitable. Due to its versatility in modeling complicated geometry, finite element method is the most widely used tool for analysis of various structural dynamics problems. Especially, for such a highly nonli-

near time-dependent problem as deployment/retraction dynamics of space structures with large change in inertia and stiffness properties, finite element method seems to be the only viable tool for theoretical analysis.

There have been many papers discussing the methods for constructing equations of motion governing the deployment of a various types of flexible appendages from a spacecraft [1-9]. The main objectives were the investigations of the effects of deploying flexible appendages on the attitude motion and stability of a spacecraft. However, in those papers, the deployment means the only extension of flexible appendages from the satellite in earth orbit and the nonlinear effects of elastic deformations were not considered. For the deployment of packaged structures, Housner [10] presented a finite element formulation for transient analysis of two dimensional beam-frame configuration in space. In his paper a convective coordinate system was used for each element because the Euler beam theory used in the formulation cannot handle large elastic deflection unless an updated coordinate system is used for individual elements. Moreover, Housner's formulation does not seem to be convenient for deployment in three dimensional space.

In this report, a finite element technique which can handle deployment of flexible structures in three dimensional space is presented. The structures is assumed to consist of a flexible bars attached to a rigid mass. The elastic deflection of bars can be very large and is coupled with gross rigid translational and rotational motions. The description of elastic deformation is based on the total Lagrangian formulation. Large deflection or rotation with respect to a body axis is handled by introducing rotational angles as independent variables for rotation of cross-sections. The equations of motion are solved timewise by a direct numerical time integration scheme using the trapezoidal rule and the Newton Raphson iteration. The parametric studies have been performed to investigate the effect of deployment on the rigid body rotational

motion. The effect of gravity gradient is also considered for the deployment of non-symmetric space structure in earth orbit.

2. EQUATIONS OF MOTION

In order to predict the motion of spacecraft with flexible bodies in earth orbit, various methods have been developed. In such a motion, large elastic deformations are coupled with the rigid body motions. The principles of conservation of linear and angular momentum are adopted to describe the gross translational and rotational motion. Also to describe the elastic deformation the principle of virtual work is used. The resulting equations of motion for elastic structures undergoing gross translational and rotational motion as well as small or large elastic deformation become a complicated set of nonlinear differential equations. Introducing finite element approximation the equations of motion can be written symbolically as follows;

$$\underset{\sim}{M}\,\ddot{\underset{\sim}{g}} + \underset{\sim}{F}_e(\underset{\sim}{g}) = \underset{\sim}{F}(\underset{\sim}{g},\dot{\underset{\sim}{g}}) \tag{2.1}$$

Note that $\underset{\sim}{g}$ denotes the nodal displacements including the gross translational and rotational displacements of body axes and elastic displacement with respect to the body axes. The dot ($\cdot$) means the time derivative. The details of $\underset{\sim}{M}$, $\underset{\sim}{F}_e$, and $\underset{\sim}{F}$ matrices are derived in reference 15.

Equation (2.1) may represent any type of structures. However, in the present study, we are interested in the development of space structures which consist of straight beams connected by hinge joints. The beam is assumed to experience small strain but large rotations are allowed. This is done by allowing transverse shear deformation and adopting the total Lagrangian description for the geometry and kinematics of deformation. The cross-section of the beam is circular therefore the cross-section is free of warping. As stated in

the previous section, with the present formulation, the kinematics of beam deformation can be described with respect to a single body axis system. The particular element used in the present study is the three node element as shown in Fig. 1. Each node has three translational displacement and three rotational angles as nodal degrees of freedom. Detailed formulation is given in Reference 15.

3. NUMERICAL INTEGRATION SCHEME

3.1 Time Integration Method

There are many methods which can be used for numerical time integration of Eq. (2.1) [13,14]. Generally these methods are classified as either explicit or implicit schemes. Explicit schemes are computationally simple but the time step size is limited by stability consideration. Implicit schemes require more computation per time step but time step size limitation are much less stringent. In the present study an implicit scheme based on the trapezoidal rule has been used.

Assuming all the variables in Eq. (2.1) are known at time $t = t_n$, the equation at time $t_{n+1} = t_n + \Delta t$ is written as

$$\underset{\sim}{M}^{n+1}\,\ddot{\underset{\sim}{q}}^{n+1} + \underset{\sim}{F}_e^{n+1} = \underset{\sim}{F}^{n+1} \tag{3.1}$$

where

$$\underset{\sim}{q}^{n+1} = \underset{\sim}{q}(t_{n+1}) \tag{3.2}$$

$$\underset{\sim}{M}^{n+1} = \underset{\sim}{M}(\underset{\sim}{q}^{n+1}) \tag{3.3}$$

$$\underset{\sim}{F}_e^{n+1} = \underset{\sim}{F}_e(\underset{\sim}{q}^{n+1}) \tag{3.4}$$

$$\underset{\sim}{F}^{n+1} = \underset{\sim}{F}(\underset{\sim}{q}^{n+1}) \tag{3.5}$$

Using trapezoidal rule

$$\underset{\sim}{q}^{n+1} = \underset{\sim}{q}^n + \frac{\Delta t}{2}\,(\dot{\underset{\sim}{q}}^n + \dot{\underset{\sim}{q}}^{n+1}) \tag{3.6}$$

$$\dot{g}^{n+1} = \dot{g}^{n} + \frac{\Delta t}{2} (\ddot{g}^{n} + \ddot{g}^{n+1}) \tag{3.7}$$

Combining Eq. (3.6) and Eq. (3.7) results in

$$g^{n+1} = \frac{4}{(\Delta t)^2} (g^{n+1} - g^{n}) - \frac{4}{\Delta t} \dot{g}^{n} - \ddot{g}^{n} \tag{3.8}$$

Substituting Eq. (3.8) into Eq. (3.1) yields

$$\underset{\sim}{M}^{n+1} [\frac{4}{(\Delta t)^2} (g^{n+1} - g^{n}) - \frac{4}{\Delta t} \dot{g}^{n} - \ddot{g}^{n}] + \underset{\sim}{F}_e^{n+1} = \underset{\sim}{F}^{n+1} \tag{3.9}$$

Eq. (3.9) is a nonlinear equation and can be solved by the Newton-Raphson iteration. Letting subscript i denote the i^{th} iteration number, Eq. (3.9) becomes as follows;

$$\underset{\sim}{M}_i^{n+1} [\frac{4}{(\Delta t)^2} (g_{i+1}^{n+1} - g^{n}) - \frac{4}{\Delta t} \dot{g}^{n} - \ddot{g}^{n}] + \underset{\sim}{F}_e(g_{i+1}^{n+1}) = \underset{\sim}{F}_i^{n+1} \tag{3.10}$$

As given in reference 15, $\underset{\sim}{F}_e$ can be decomposed into

$$\underset{\sim}{F}_e (g_{i+1}^{n+1}) = \underset{\sim}{K}_{T_i}^{n+1} \Delta g^{n+1} + \underset{\sim}{F}_{S_i}^{n+1} \tag{3.11}$$

where

$$\Delta \underset{\sim}{q}_i^{n+1} = g_{i+1}^{n+1} - g_i^{n+1}$$

Note that the $\underset{\sim}{K}_T$ is the tangential stiffness matrix and $\underset{\sim}{F}_S$ is the initial stress force vector. Using Eq. (3.11), Eq. (3.10) can be written as follows;

$$\underset{\sim}{K}_i^{*} \Delta g_i^{n+1} = \underset{\sim}{F}_i^{*} \tag{3.12}$$

where

$$\underset{\sim}{K}_i^{*} = \underset{\sim}{K}_{T_i}^{n+1} + \frac{4}{\Delta t} \underset{\sim}{M}_i^{n+1} \tag{3.13}$$

$$\underset{\sim}{F}_i^{*} = \underset{\sim}{F}_i^{n+1} - \underset{\sim}{M}_i^{n+1} g_i^{n+1} - \underset{\sim}{F}_{S_i}^{n+1} \tag{3.14}$$

In order to start the iteration the state of the structure at time t_n is used as a first approximation to the state of structure at time t_{n+1} for all the terms except $\underset{\sim}{F}_S^{n+1}$. Since the mass and stiffness matrices change slowly with

time, above assumption is adequate for the first estimation of these terms. Because $\underset{\sim}{F}_S^{n+1}$ is a nonlinear function of both $\underset{\sim}{g}^{n+1}$ and $\dot{\underset{\sim}{g}}^{n+1}$, however, the following predictors are used to ensure the stability of solution [12].

$$\overline{\underset{\sim}{g}}^{n+1} = \underset{\sim}{g}^n + \Delta t\, \dot{\underset{\sim}{g}}^n + \frac{\Delta t^2}{4} \ddot{\underset{\sim}{g}}^n \tag{3.15}$$

$$\dot{\overline{\underset{\sim}{g}}}^{n+1} = \dot{\underset{\sim}{g}}^n \quad \frac{\Delta t}{2} \ddot{\underset{\sim}{g}}^n \tag{3.16}$$

Note that Eqs. (3.15) and (3.16) are obtained by setting $\ddot{\underset{\sim}{g}}^{n+1} = 0$ in Eqs. (3.6) and (3.7). For subsequent iterations, the displacment, velocity and acceleration are corrected by Eqs. (3.6) ~ (3.8).

The iterations continue until Δg_i^{n+1} converges to within the preassigned tolerance Λ, that is,

$$\left\| \frac{\Delta g_i^{n+1}}{g_i^{n+1} - g^n} \right\| < \Lambda$$

where $\|.\|$ is the Euclidean norm of '$\cdot$'. For the problems considered here, $\Lambda = 0.01$.

3.2 Constraint Conditions

The deployment procedure adopted in the present study models a method described in Reference 11 in which a pushrod is connected to two adjacent bars to transfer torque across the hinge. The deployment is accomplished by means of driving a pushrod link. For this, it is reasonable to treat the relative angles between two adjacent bars as a prescribed quantity. Assuming deployment in a plane for the sake of simplicity, the constraint conditions are given as

$$q_j - q_i = \theta \tag{3.17}$$

where

q_i, q_j are nodal rotational angles with $j > i$

θ is the prescribed relative angle in radians

Using Eq. (3.19), the nodal displacement vector $\underset{\sim}{q}$ can be written as

$$\underset{\sim}{q} = \begin{Bmatrix} q_1 \\ \vdots \\ q_i \\ \vdots \\ q_j \\ \vdots \\ q_n \end{Bmatrix} = \begin{Bmatrix} q_1 \\ \vdots \\ q_i \\ \vdots \\ q_i+\theta \\ \vdots \\ q_n \end{Bmatrix}$$

$$= \underset{\sim}{T}_B \begin{Bmatrix} q_1 \\ \vdots \\ q_i \\ \vdots \\ \theta \\ \vdots \\ q_n \end{Bmatrix} \equiv \underset{\sim}{T}_B \, g^* \qquad (3.18)$$

where

$\underset{\sim}{T}_B$: n x n matrix with $T_{ji} = 1$, $T_{ii} = 1$ and all other components =0

$g^{*T} = \lfloor q_1 \; .. \; q_i \; .. \; \theta \; .. \; q_n \rfloor$

Since θ is a given value, the virtual displacement vector δg^* can be transformed as follows;

$$\delta g = \underset{\sim}{T}_B \begin{Bmatrix} \delta q_1 \\ \vdots \\ \delta q_i \\ \vdots \\ 0 \\ \vdots \\ \delta q_n \end{Bmatrix} \equiv \underset{\sim}{T}_B \, \delta g^* \qquad (3.19)$$

The equations of motion Eq. (3.1) in virtual work form can be written symbolically as follows;

$$\delta g^T (\underset{\sim}{M} \ddot{g} + \underset{\sim}{K} g - \underset{\sim}{F}) = \underset{\sim}{0} \qquad (3.20)$$

Substituting Eqs. (3.18) and (3.19) into Eq. (3.20) results in

$$\delta g^{*T} (\underset{\sim}{T}_B^T \underset{\sim}{M} \underset{\sim}{T}_B \ddot{g} + \underset{\sim}{T}_B^T \underset{\sim}{K} \underset{\sim}{T}_B g^* - \underset{\sim}{T}_B^T \underset{\sim}{F}) = \underset{\sim}{0} \qquad (3.21)$$

To satisfy the Eq. (3.21) for arbitrary δg^*, then

$$\underset{\sim}{M}^* \ddot{\underset{\sim}{g}}^* + \underset{\sim}{K}^* \underset{\sim}{g}^* = \underset{\sim}{F}^* \tag{3.22}$$

where

$$\underset{\sim}{M}^* = \underset{\sim}{T}_B^T \underset{\sim}{M} \underset{\sim}{T}_B \tag{3.23}$$

$$\underset{\sim}{K}^* = \underset{\sim}{T}_B^T \underset{\sim}{K} \underset{\sim}{T}_B \tag{3.24}$$

$$\underset{\sim}{F}^* = \underset{\sim}{T}_B^T \underset{\sim}{F} \tag{3.25}$$

4. NUMERICAL TEST

Numerical tests were carried out to check the validity of the present formulation. For simplicity two simple deployments in two dimensional plane was chosen as example problems. The structure is assumed to consist of a rigid mass and a series of flexible bars connected through joints.

4.1 Case 1

Fig. 2 shows deployment of flexible bars attached to a rigid body. The center of mass of the rigid body is restrained against any translational motion. However, it is allowed to rotate around the fixed point. It is assumed that initially the folded bars are aligned along the x axis. The material properties used in the calculation are mass density $\rho = 3 \times 10^{-3}$ slug/in^3, Young's modulus $E = 10 \times 10^6$ psi, and shear modulus $G = 3.85 \times 10^6$ psi. The total mass of the elastic bars is 100 slugs. The time required to deploy from the initial folded configuration to fully deployed state is chosen to be 100 seconds. The deployment schedule is assumed as follows;

$$\theta(t) = \frac{\pi}{T_d} t - \sin\left(\frac{2\pi}{T_d} t\right) \qquad \text{(radians)}$$

Note that $\theta(t)$ is the relative angle at the joint between two adjacent bars and T_d is the time required for the completion of deployment to $\theta = 180°$.

In order to observe the effect of deployment on the rotational motion of the rigid mass, parametric studies were performed. First, while the total mass of bars kept constant, the length of bars was varied. Of course this results in changes in the cross-sectional properties such as area and moment of inertia etc. Two different lengths were considered. They are $L_1 = 300\sqrt{2}$ ft and $L_2 = 300\sqrt{3}$ ft. The cross-sectional properties corresponding to $L = 300\sqrt{2}$ are area $A = 4.56 \times 10^{-2}$ ft^2, cross-sectional area moment of inertia $I = Iyy = Izz = 2.89 \times 10^{-3}$ ft^4. Next the ratio of rotary inertia, IRATIO, was introduced as a parameter as follows;

$$\text{IRATIO} = \frac{\text{Rotary moment of inertia of fully deployed bars}}{\text{Rotary moment of inertia of rigid mass}}$$

The rotary moment of inertia was defined with respect to the center of rigid mass. In the present calculation, the values of IRATIO were chosen as 1 and 5. The number of flexible bars were either two or three.

Figures 3 to 5 show the rotational angle of rigid mass vs. time up to 200 seconds. In all cases, the effect of flexibility of the bars are small in the initial stage of deployment. However the difference between the rigid bar model and the elastic bar model increases as time progresses. As shown in the figures the difference is quite substantial after the completion of deployment (t = 100 secs). For a fixed rotary inertia ratio, the rigid mass with longer bars ($L = 300\sqrt{3}$) experiences a wider excursion of rotational angles than the one with shorter bars ($L = 300\sqrt{2}$). With a fixed L, the higher rotary inertia ratio (IRATIO = 5) case shows more pronounced effect than the lower ratio (IRATIO = 1 case) as expected. For the same IRATIO and L, the trend for the three-bar case is similar to that for the two-bar case. However the three-bar case shows less effect of flexibility.

4.2 Case 2 - Deployment in Earth Orbit

This problem is exactly the same as that in the previous section section except that now the fictitious space structure is assumed to be in a 200 mile circular orbit around the earth. The folded bars are initially aligned in the direction of the velocity vector tangent to the circular orbit. In the calculation, the ratio of rotary inertia was fixed as IRATIO = 5. Instead, a mass ratio (MRATIO) was introduced as follows:

$$\text{MRATIO} = \frac{\text{total mass of the bars}}{\text{mass of the rigid body}}$$

The MRATIO was chosen as either 0.2 or 0.5.

The plots of rotational angle vs. time of two-bar case are shown in Figures 6 and 7, which have almost same trends as Fig. 3. Because the gravity gradient tends to align the structure with the radial direction, however, the effects of deployment on rotational motion are reduced. It shows that, with the fixed IRATIO, the higher mass ratio (MRATIO = 0.5) case is subject to the more gravity effect than the lower ratio (MRATIO = 0.2). Figures 8 and 9 show the results of three-bar case. They also show the same tendency as the previous case.

5. CONCLUSION

A finite element modeling and solution techniques was developed for flexible space structures undergoing large timewise change in inertia and stiffness properties as a result of change in geometrical configuration during deployment and retraction maneuvers. Simple numerical tests and parametric studies demonstrate the validity of the present formulation and the effect of flexibility on the rotational motion of the rigid mass.

The present formulation is based on the total Lagrangian description for the description of deformation of flexible bars. In addition, cross-sections of bars are allowed to undergo arbitrary rotation in three-dimensional space. This permits the description of motion of the flexible bars with respect to a simple axis system attached to the rigid mass or any point in the structure.

REFERENCES (PART 2)

1. Cloutier, G.J., "Dynamics of Deployment of Extendible Booms from Spinning Space Vehicles," J. of Spacecraft and Rockets, Vol. 5, No. 5, May 1968, pp. 547-552.

2. Sellappan, R. and Banium, P.M., "Dynamics of Spin Stabilized Spacecraft During Deployment of Telescoping Appendage," J. of Spacecraft and Rockets, Vol. 13, No. 10, Oct. 1976, pp. 605-610.

3. Lips, K.W. and Modi, V.J., "Three-Dimensional Response Characteristics for Spacecraft with Deploying Flexible Appendages," J. of Guidance and Control, Vol. 4, No. 6, 1981, pp. 650-656.

4. Lips, K.W. and Modi, V.J., "Transient Attitude Dynamics of Satellites with Deploying Flexible Appendages," Acta Astronautics, Vol. 5, 1978, pp. 797-815.

5. Ibrahim, A.E. and Misra, A.K., "Attitude Dynamics of a Satellite During Deployment of Large Plate-Type Structures," J. of Guidance and Control, Vol. 5, No. 5, 1982, pp. 442-447.

6. Tsuchiya, K., "Dynamics of a Spacecraft During Extension of Flexible Appendages," J. of Guidance and Control, Vol. 6, No. 2, 1983, pp. 100-103.

7. Lips, K.W. and Modi, V.J., "Dynamics of a Deploying Orbiting Beam-Type Appendage Undergoing Librations," J. of Vibration,, Acoustics, and Reliability in Design, Vol. 105, Jan. 1983, pp. 33-39.

8. Djerassia, S. and Kane, T.R., "Equations of Motion Governing the Deployment of a Flexible Linkage from a Spacecraft," J. of Astronautical Sciences, Vol. 33, No. 4, 1985, pp. 417-428.

9. Cherchas, D.B., "Dynamics of Spin-Stabilized Satellites During Extension of Long Flexible Booms," J. of Spacecraft and Rockets, Vol. 8, Jul. 1871, pp. 802-804.

10. Housner, J., "Convected Transient Analysis for Large Space Structures Maneuver and Deployment," AIAA 84-1023, pp. 616-629.

11. Sullivan, M.R., "LSST (Hoop/Column) Maypole Antenna Development Program," NASA CR 3558, Jun. 1982.

12. Hughes, T.J.R., Pister, K.S. and Taylor, R.L., "Implicit-Explicit Finite Element in Nonlinear Transient Analysis," Computer Method in Applied Mechanics and Engineering, Vol. 17/18, Mar. 1979, pp. 159-182.

13. Felippa, C.A. and Park, K.C., "Direct Time Integration Methods in Nonlinear Structural Dynamics," Computer Methods in Applied Mechanics and Engineering, Vol. 17/18, 1979, pp. 277-313.

14. Belytschko, T., "A Survey of Numerical Methods and Computer Programs for Dynamic Structural Analysis," Nuclear Engineering and Design, Vol. 37, 1976, pp. 23-24.

15. Christensen, E.R., "Development of a Dynamic Finite Element Model for Unrestrained Flexible Structures," Ph.D. Dissertation, University of Maryland, 1984.

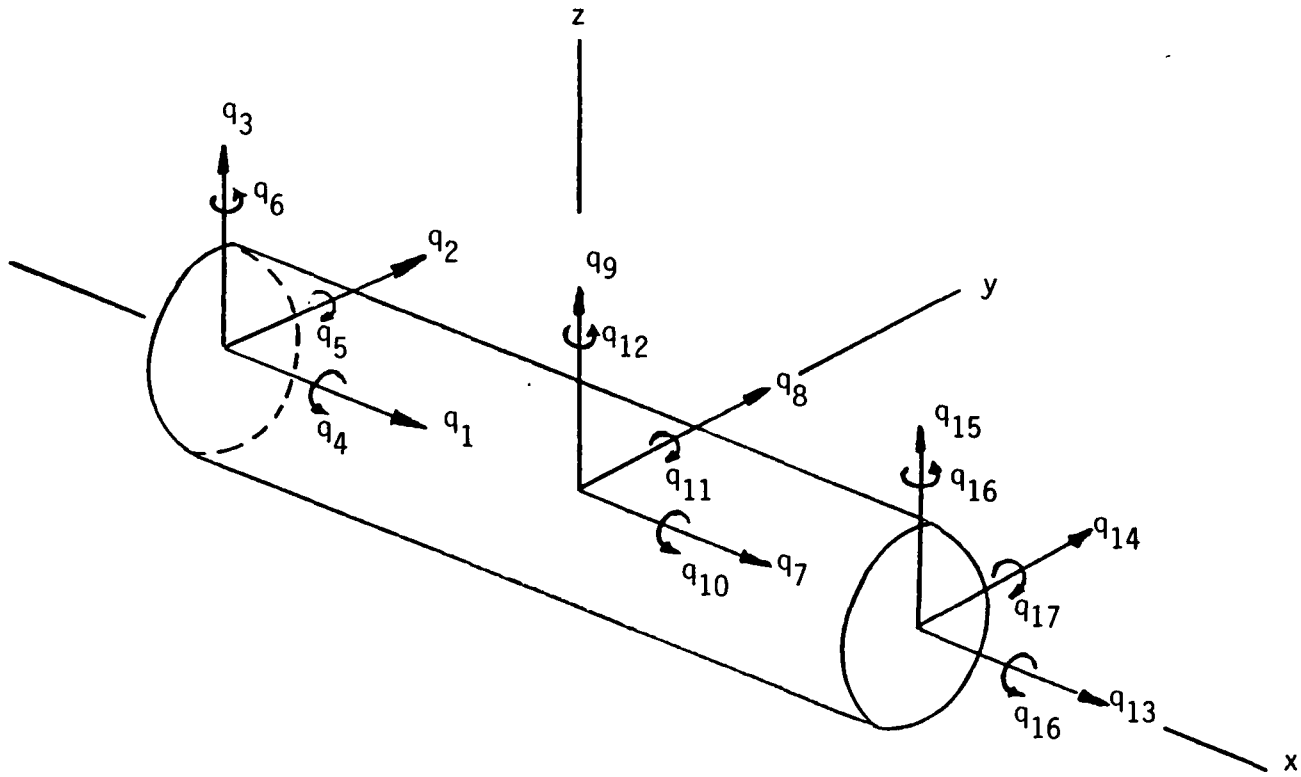

Fig. 1 Three Node Eighteen Degrees of Freedom Beam Element

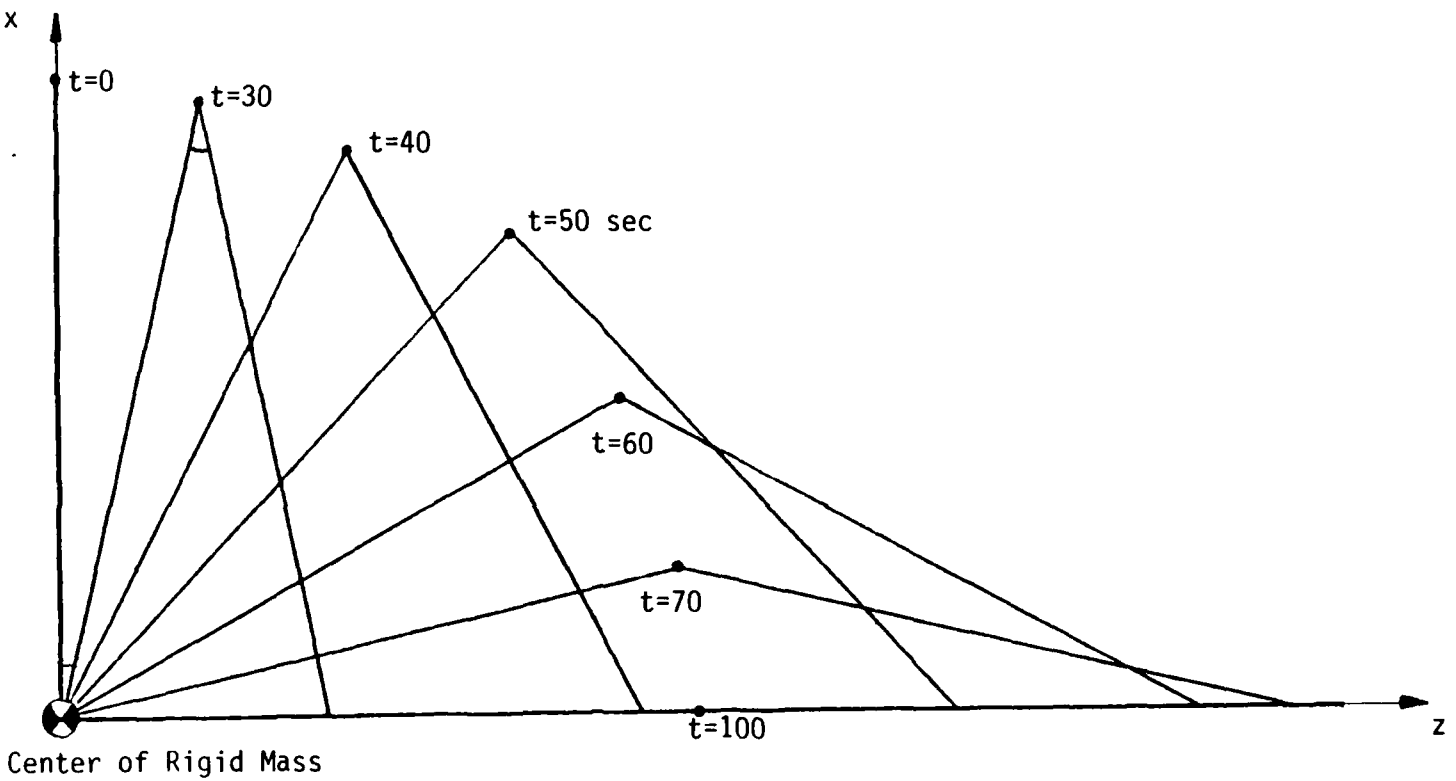

Fig. 2 Deployment Sequence of Two Bars attached to a Rigid Mass

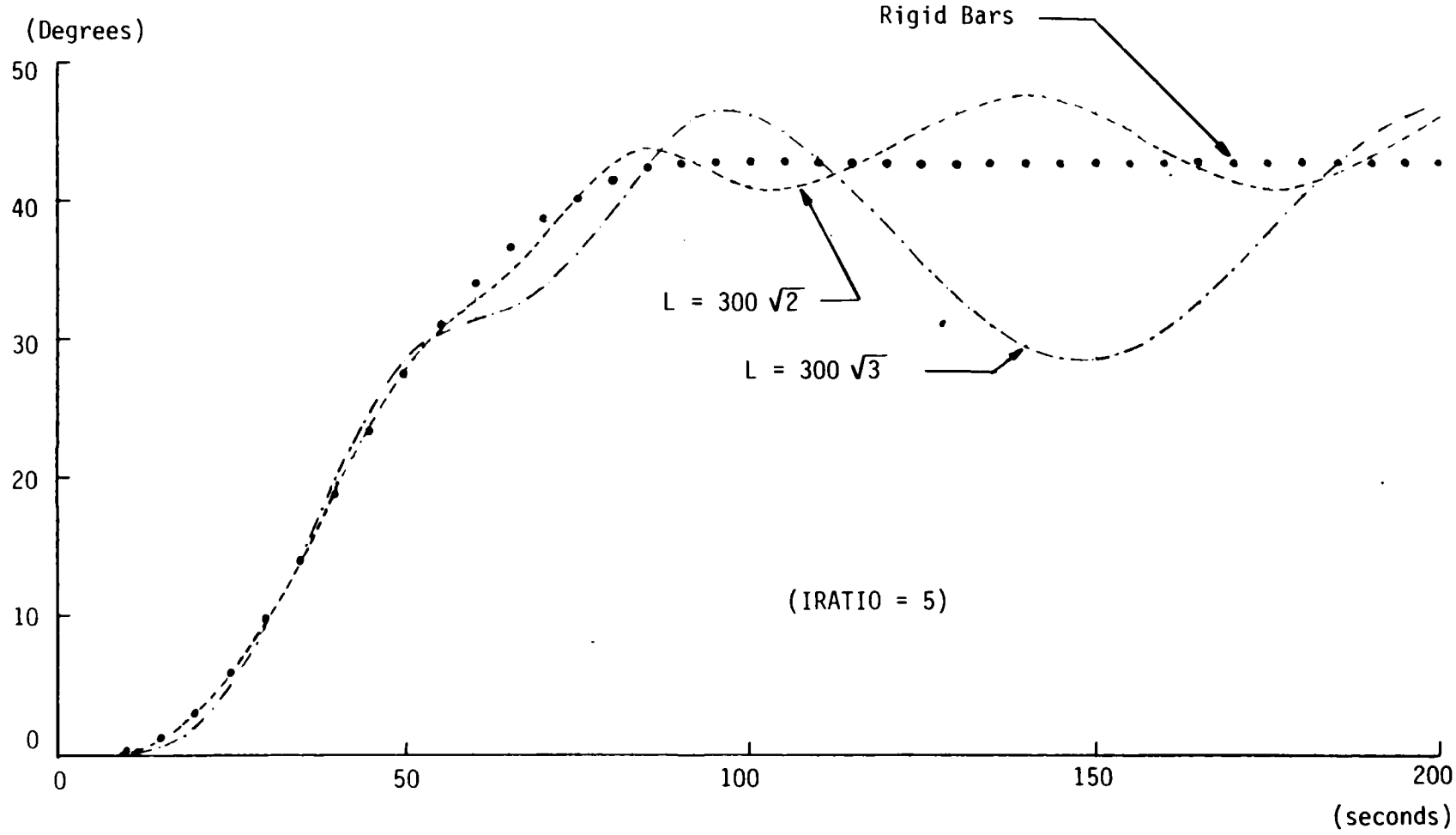

Fig. 3 Rotational Angle of the Rigid Mass vs. Time (2-Bar Deployment)

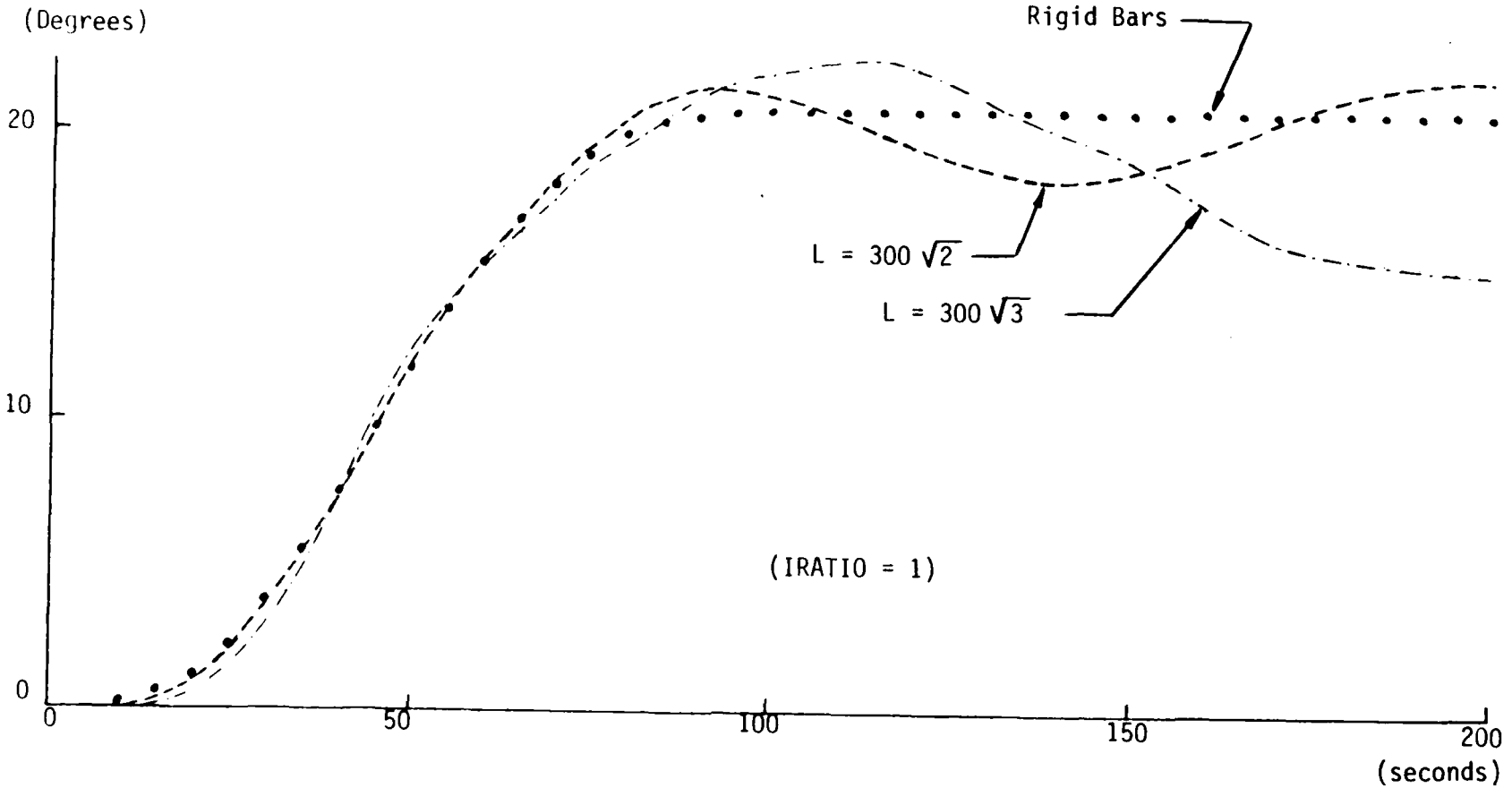

Fig. 4 Rotational Angle of the Rigid Mass vs. Time (2-Bar Deployment)

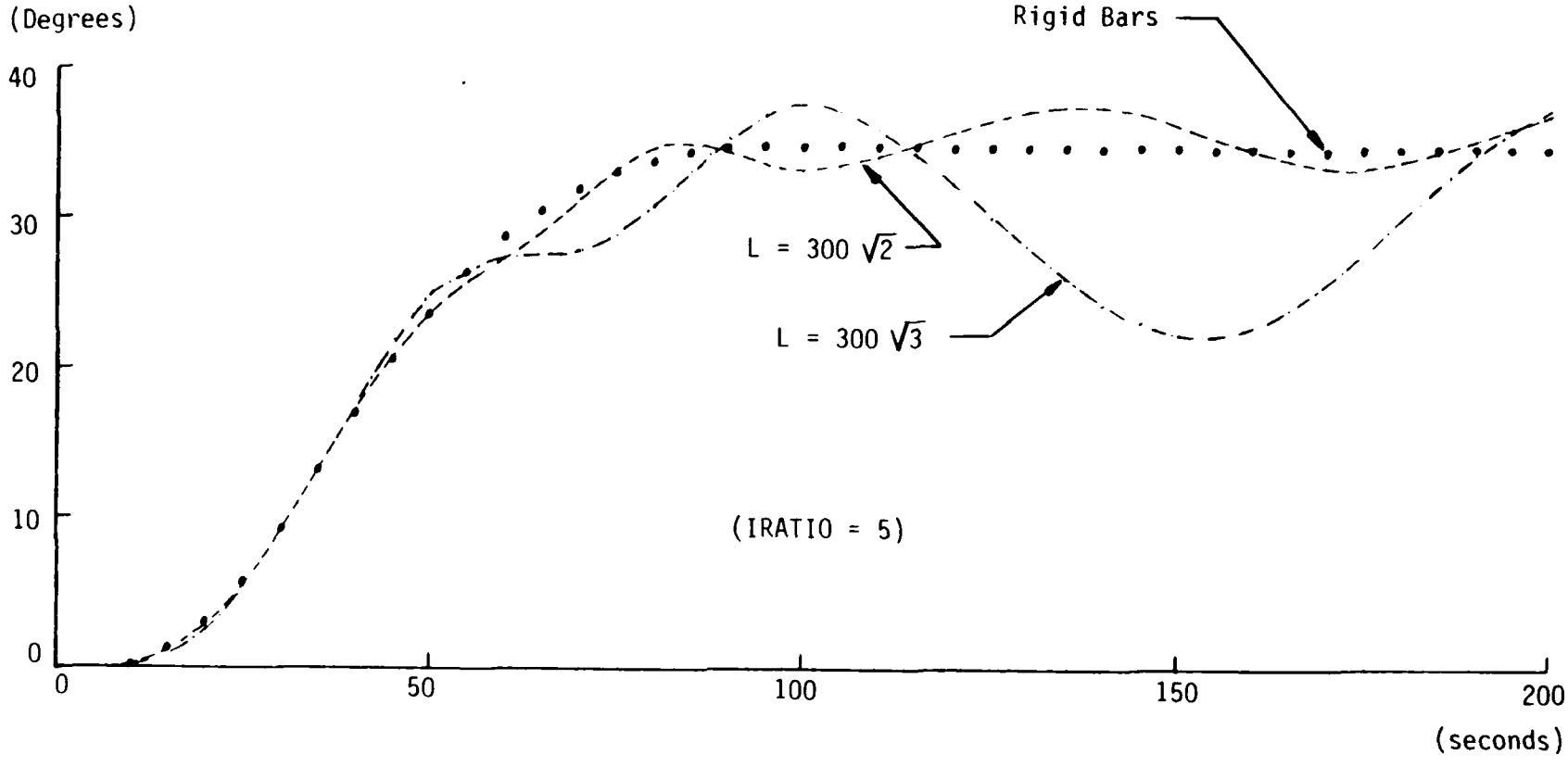

Fig. 5 Rotational Angle of the Rigid Mass vs. Time (3-Bar Deployment)

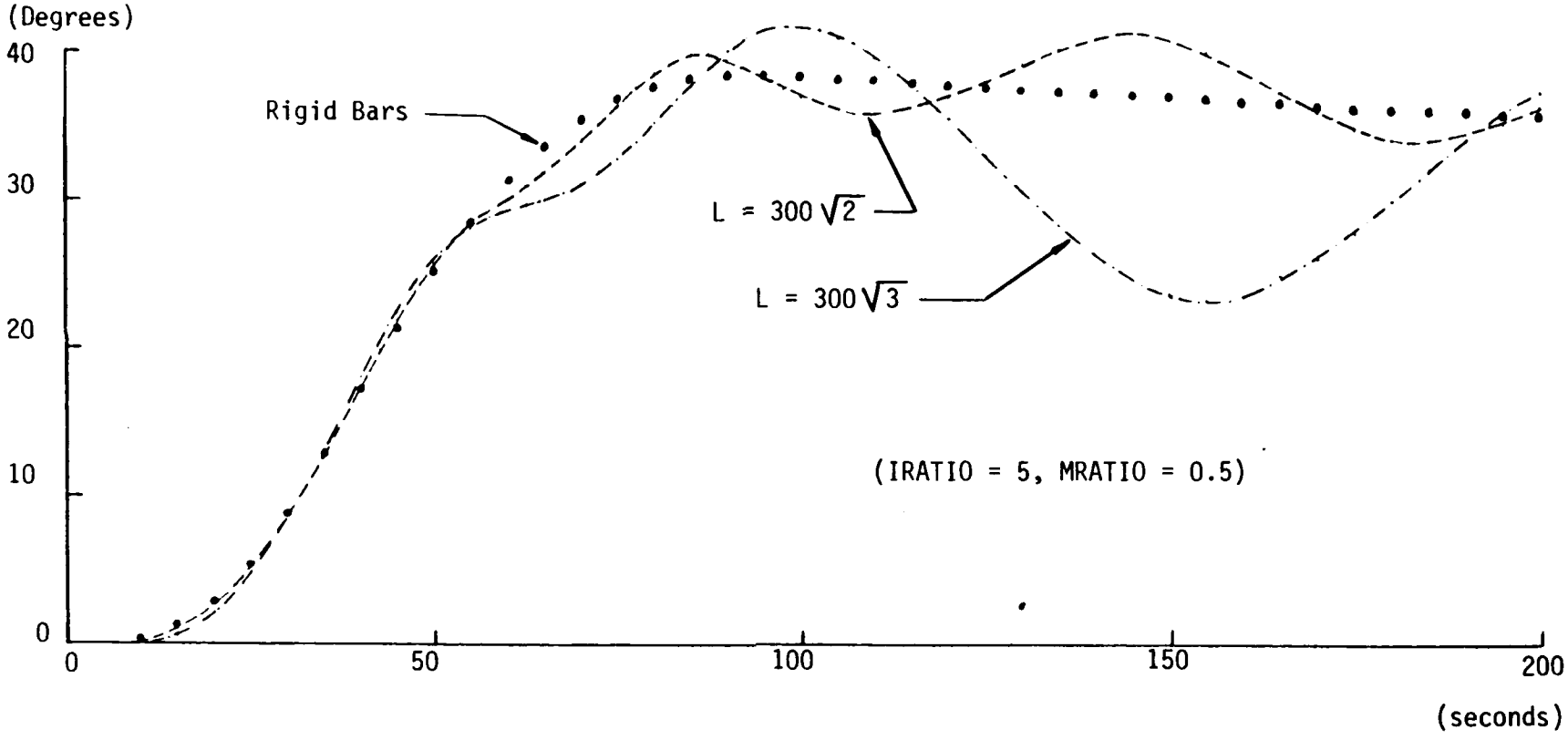

Fig. 6 Rotational Angle of the Rigid Mass vs. Time (2-Bar Deployment in Orbit)

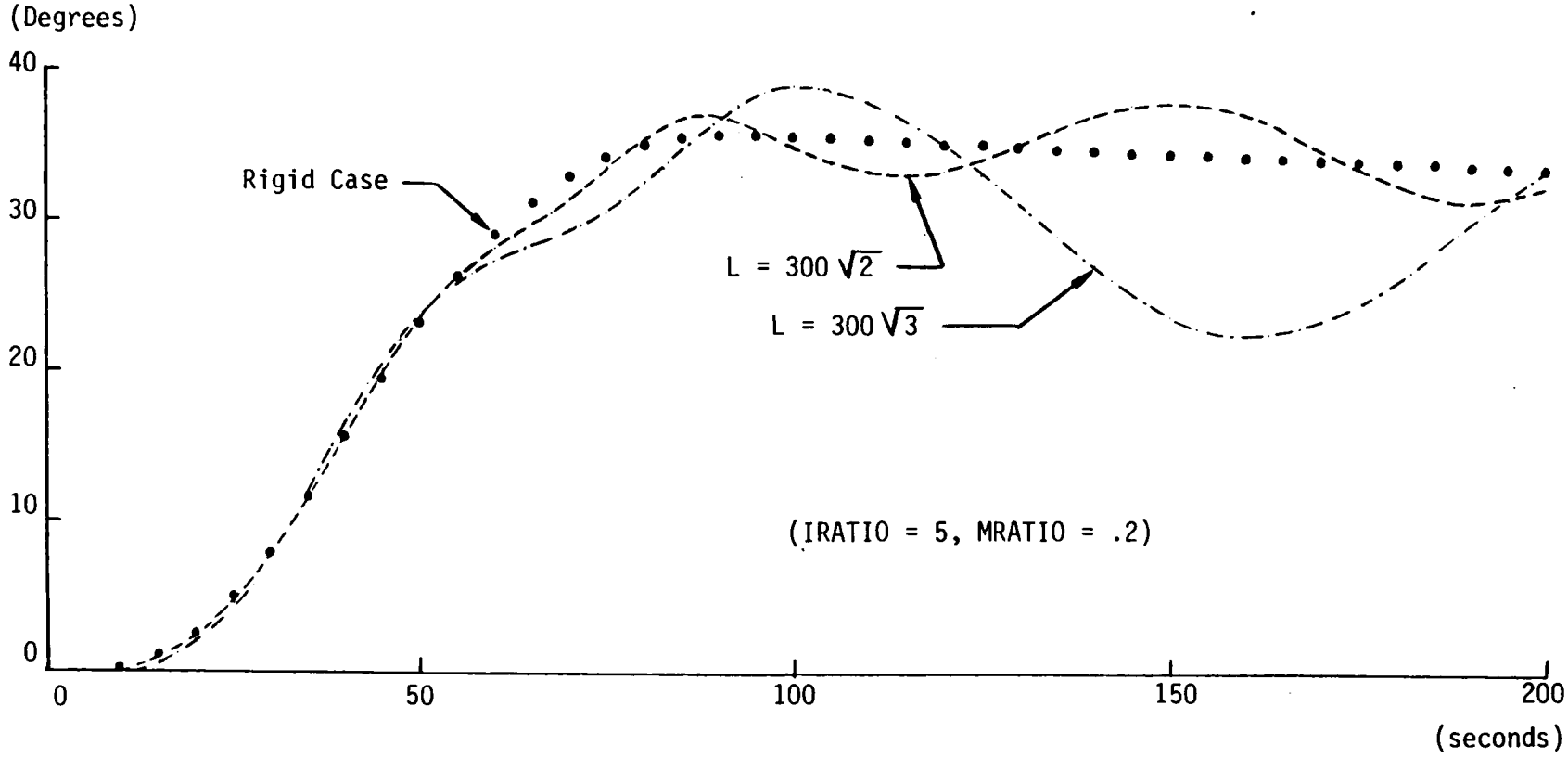

Fig. 7 Rotational Angle of the Rigid Mass vs. Time (2-Bar Deployment in Orbit)

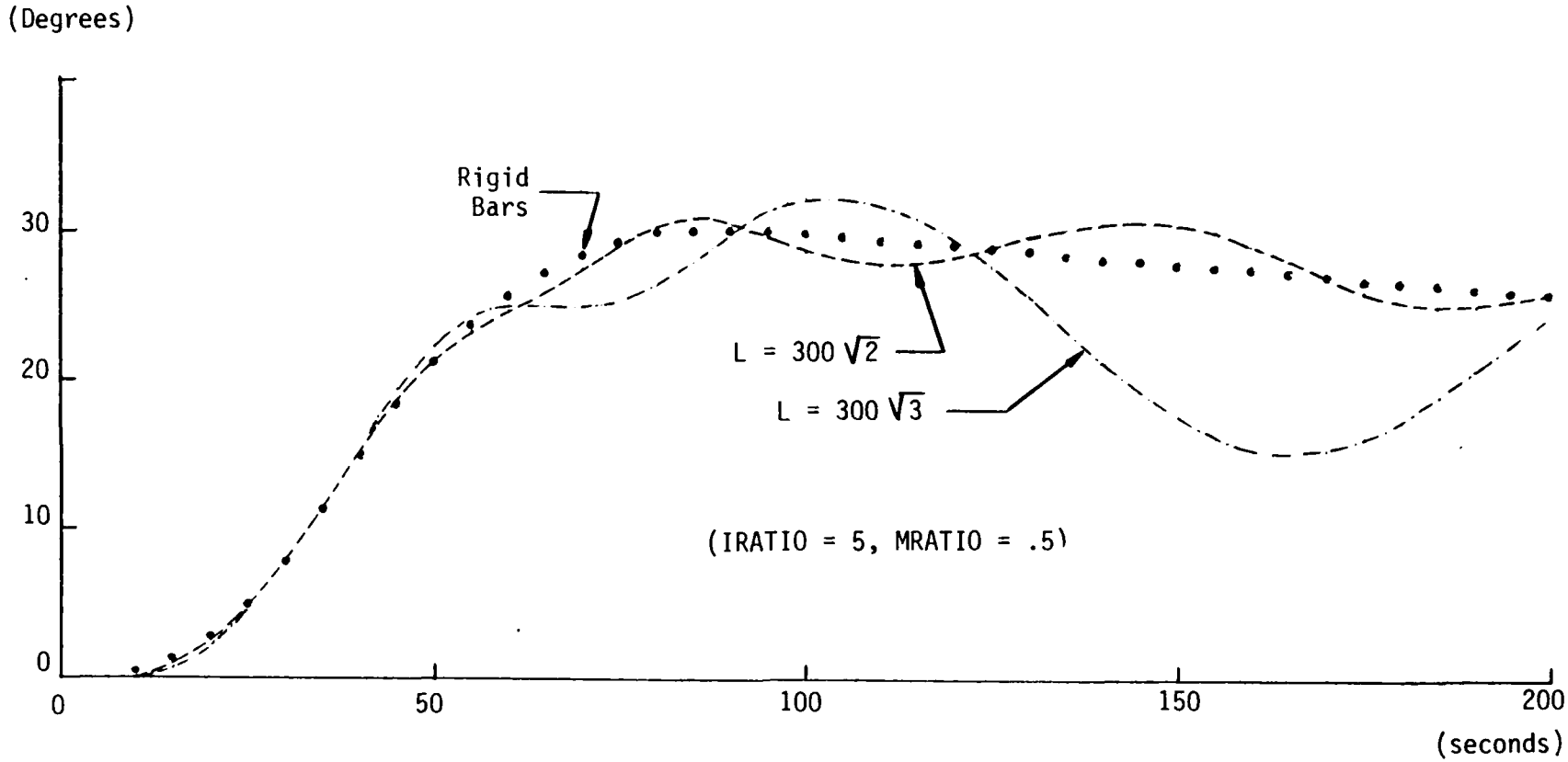

Fig. 8 Rotational Angle of the Rigid Mass vs. Time (3-Bar Deployment in Orbit)

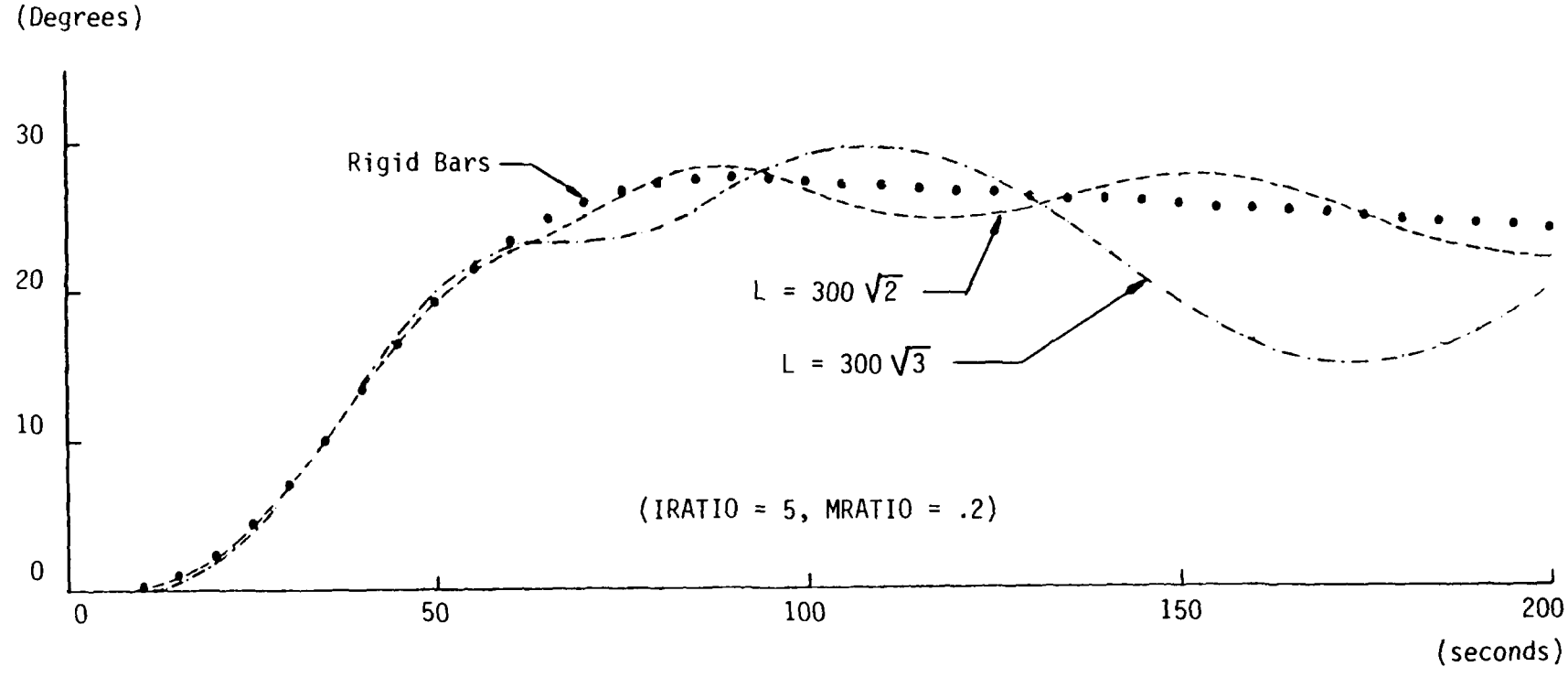

Fig. 9 Rotational Angle of the Rigid Mass vs. Time (3-Bar Deployment in Orbit)

END

3-87

DTIC